PHYSICAL REVIEW B **77**, 165304 (2008)

Recombination at heterojunctions in disordered organic media: Modeling and numerical simulations

Ivan Jurić,[1,*] Ivo Batistić,[2] and Eduard Tutiš[1,†]

[1]*Institute of Physics, Bijenička c. 46, P.O. Box 304, HR-10001 Zagreb, Croatia*

[2]*Department of Physics, University of Zagreb, Bijenička c. 32, P.O. Box 331, HR-10002 Zagreb, Croatia*

(Received 30 October 2007; revised manuscript received 25 January 2008; published 2 April 2008)

Multilayer organic electroluminescent devices derive their advantages over their single-layer counterparts from the processes occurring at heterojunctions in organic media. These processes significantly differ from those in the bulk of the material. This paper presents three-dimensional modeling, numerical simulations, and a discussion of transport and recombination in a system with a heterojunction. We consider partial cross sections for the creation of excitons and exciplexes, and probabilities for recombination in the respective channels. We examine the influence of the energy barrier, electric field, site-energy disorder, and structural disorder at an organic-organic interface on transport and recombination. In particular, we investigate optimal parameter domains for recombination in the exciton channel. The interface roughness, unlike the site-energy disorder, is found to strongly affect the partial cross sections.

DOI: 10.1103/PhysRevB.77.165304 PACS number(s): 73.50.Gr, 73.40.Lq, 85.60.Jb, 72.80.Le

I. INTRODUCTION

The past decades have been marked by significant advances in the construction of new light sources and screens. Recently, organic light emitting diodes (OLED) came under the spotlight;[1] they are characterized by the relatively simple construction and variety of organic compounds available for their assembly. As is the case with their inorganic cousins, light in OLEDs is obtained through recombination of injected electrons and holes. Unlike in classical semiconductors, in organic molecular media the charge carriers move by phonon-assisted hops among well-localized molecular states, thus suffering from much lower mobility.[2–9] Another difference is that the exciton state forms essentially on a single molecule.[10] It subsequently deexcites by emitting a photon or molecular vibrations. In the simplest terms, efficient light production requires a successful preparation of excitons on molecules of the luminescent material.

The prerequisites for an efficient device differ in the two prominent types of OLEDs: single-layer devices and bilayer devices. In the single-layer OLEDs, recombination takes place throughout the device. The rate of recombination is given, to a good approximation by the well-known Langevin bimolecular formula,[11–13]

$$R \equiv j_n \sigma_L p + j_p \sigma_L n = \gamma_L n p. \tag{1}$$

Here, R denotes the recombination rate density, n and p are particle densities of electrons and holes, and j_n and j_p are the respective current densities. $\sigma_L = q_e/\varepsilon_0 \varepsilon_r F$ is the *cross section* for an electron reaching a hole while drifting under the influence of the homogeneous external field F and Coulomb potential of the hole. The recombination constant γ_L in Eq. (1) thus depends on the relative mobility, $\mu \equiv \mu_n + \mu_p$, of electrons and holes in the medium, $\gamma_L = \mu q_e/\varepsilon_0 \varepsilon_r$.

High efficiency in single-layered devices requires a well-matched overlap of the electron and hole densities throughout the device, implying well-matched injection characteristics at the cathode and anode.[12] This requirement is relaxed in the bilayer OLEDs, as well as in their multilayer generalizations, where modified recombination circumstances are able to compensate for unbalanced electrodes. In bilayer OLEDs, two materials of different highest occupied molecular orbital (HOMO) and lowest unoccupied molecular orbital (LUMO) levels are brought into contact. This introduces an energy barrier at the heterojunction that impedes transport and favors recombination. The usual picture has been that the energy barrier causes a large accumulation of holes and electrons at opposite sides of the heterojunction.[14] The recombination rate, calculated through Eq. (1), profits from the increased density of carriers. Thus, the accumulation of carriers has long been regarded as the prime reason for a large increase of the recombination rate in bilayers.

Recently, Greenham and Bobbert have pointed out that this picture is essentially incorrect.[15] The motion of carriers near the heterojunction differs significantly from the motion in the bulk. In particular, the mobilities entering the expression for γ_L are ill-defined near the sharp border separating two materials. Greenham and Bobbert pointed to a correlated behavior of electrons and holes at the heterojunction. They focused on the attraction of a single electron and a single hole, showing that their motion within the heterojunction plane greatly increases the probability of recombination, thereby also drastically reducing the density of carriers required at the heterojunction to sustain the current imposed by the electrodes. The most important implications on device modeling were demonstrated in a simplified model of a bilayer device.[15] We also comment on these implications toward the end of this paper.

In terms of Eq. (1), it is the cross section for the recombination process that greatly increases when an energy barrier is imposed. As is detailed later on, the augmentation of the cross section is a consequence of the anisotropy introduced in the heterojunction: a charge carrier moves much more easily along the heterojunction plane than through it. The beneficial influence of anisotropy on the recombination has been considered, to some extent, in the existing literature. For example, Gartstein *et al.*[13] studied a homogeneous system (bulk) in which mobility was anisotropic in space.

They showed that the anisotropy may increase the recombination cross section, although the effect can be reduced by disorder. It should be noted, however, that the problem treated by Gartstein *et al.* differs from the heterojunction problem, both in terms of physical origin of the anisotropy (property of a single material vs the effect of two materials in contact) and mathematically (anisotropy homogeneous vs localized in space). Nevertheless, it is possible and convenient to extend both the language and the method of Gartstein *et al.* to the heterojunction problem. In particular, it is convenient to use the recombination cross section as a measure of success of the heterojunction in emphasizing recombination over bare transport. Furthermore, one may introduce partial cross sections to account for various recombination channels. We take this approach in the paper to calculate the recombination cross sections in the system with a heterojunction and study their dependence on several parameters characterizing the system.

Our treatment of the heterojunction goes beyond that of Greenham and Bobbert in several ways. First, we consider a full three-dimensional problem of carrier motion both far from and near the heterojunction. Second, the hopping processes parallel and perpendicular to the barrier are taken on an equal footing for arbitrary barrier height. This makes it possible for us to consider the dependence over a range of barrier heights, from very low barriers, where we reproduce the bulk recombination, up to very high barriers that cannot be passed without direct assistance of a carrier of the opposite sign. Third, the possibility of crossing the heterojunction without subsequent recombination is naturally accounted for in our approach. Fourth, we consider creation and recombination of the excitons and the exciplexes separately, a distinction that is essential for an appropriate description of the organic-organic interface and the spectrum of the emerging light. Finally, we explicitly consider the spatial variation of the effective barrier caused by the Coulomb interaction between the electron and the hole. The reduction of the barrier at short distances from the hole affects the crossing as well as the formation probability and the nature of the bound state.

In this paper, we replace the Monte Carlo approach of Gartstein *et al.* with a master equation approach without altering the problem mathematically.[16] The master equation approach also directly provides the average particle flow far from and near the recombination center, which is quite useful for a visualization of the physics involved.

II. MODEL AND METHOD

Before we turn to the exposition of the model, the reader should be reminded of extensive literature that explores the nature of electronic transport in organic disordered materials through theoretical models.[17] Early works by Bässler and co-workers[18,19] concentrated on the Miller-Abrahams hopping among localized impurity states. Later papers showed that the proper description is one of a small polaron hopping in the antiadiabatic regime,[3–9,20] where the carrier is trapped at each site (molecule or conjugated segment in polymers) by coupling to the local deformation. The hopping between the sites is a multiphonon process. Numerous works have pointed to the essential role of disorder in explaining the temperature and electric field dependence of the mobility.[21–24] In realistic conditions, the disorder of local energy levels (energetic disorder) is more significant than the positional or the orientational disorder of organic units.[7,18,25] Moreover, the spatial correlation of disorder is regarded as essential for reproducing the proper field dependence of mobility.[21–23] The correlation in energy levels is induced by structural correlations and by the long-range Coulomb interactions between the carrier and the random molecular environment.[22,23,26,27]

The important role of the local molecular environment on the charge transport in the bulk gives a perspective on the importance of the heterojunction, at which the local environment is significantly altered in comparison to the interior of the material. In principle, all types of disorder (energetic, structural, stacking, etc.) and their effects have to be reexamined at the heterojunction. Many of them are not considered separately here in order to keep the paper reasonably focused. For example, we do not consider the influence of the anisotropy of the mobility in materials, which may be pronounced in polymers. Likewise, positional, orientational, and stacking disorders are not explicitly examined, although their effects may show in particular devices.[28,29] On the other hand, we do examine the effects of energetic disorder, though not to the extent previously done for the transport through homopolar heterojunctions.[30,31] The influence of the roughness of the organic-organic interface is also examined.

It is important to emphasize that the most significant results of our paper are independent of many details of the model. In essence, we show that the recombination cross section is orders of magnitude bigger than is usually assumed in device models; the effective barrier at the heterojunction for exciton creation is much lower than commonly considered; and conditions for the crossovers between regimes of no recombination/exciton-channel recombination/exciplex-channel recombination are roughly determined by Coulomb interaction between carriers located at nearby molecules. These results rely on very few assumptions in the underlying physics: the transport occurs through hopping between local states; the hopping is effectively short range and the hopping law obeys the microbalance requirement. The results are not essentially influenced either by the choice of a hopping law employed in the model or by the energetic disorder in materials. Indeed, it has been shown before that the difference in hopping laws, which greatly influences the mobility in ordered systems, becomes secondary when energy barriers dominate the transport,[23] especially near the heterojunction.[30]

We now proceed with the exposition of the model. The molecular medium is represented as a cubic grid of $N_x \times N \times N$ sites [see Fig. 1(a)]. Each site represents a molecule with spatially localized electronic states. The sites are separated by a distance a, which corresponds to the size of a molecule. The same approach has been widely used for the modeling of hopping transport in energetically disordered manifolds such as in materials used in OLEDs, both by Monte Carlo and by master equations.[2,16,23,30,32,33] Since we are dealing with fairly large organic molecules, much larger

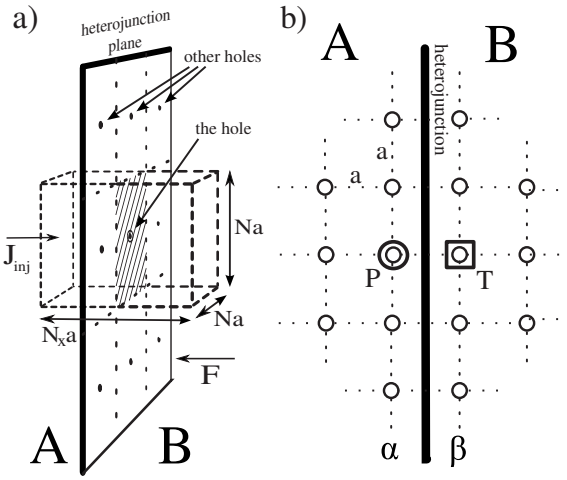

FIG. 1. Schematics of the system used in simulation. (a) Shows the heterojunction plane, separating materials A and B. The rectangular box (dashed) represents the portion of the system considered in the simulation. Electrons enter at the left-hand side of the box and exit, if not recombined, on its-right hand side. Periodic boundary conditions are imposed in the directions parallel to the heterojunction plane. There is one hole per box, positioned at the *T* site, right after the heterojunction in medium B. The hole, assumed to be immobile, attracts the incoming electron and provides an opportunity for recombination. (b) Shows a magnified view of the neighborhood of the *T* site in the plane perpendicular to the heterojunction. *P* denotes the site in material A involved in the formation of the exciplex state.

than the attenuation distance of the electron's wave function of a single molecule, only the nearest neighbor hopping is kept in the model. The hopping rules that are usually implemented in the studies of hopping transport in an organic medium are the symmetric hopping law, the Miller-Abrahams formula,[34] and the symmetric polaronic formula.[20,23,30] In several tests that we ran, the choice of law produced only minor quantitative and no qualitative differences in the results. This is to be expected from the argument presented in Ref. 30, where analytic and numerical solutions for a homopolar heterojunction are compared for three hopping laws. Here, we opt for the symmetric version of the hopping formula, where the probability for the hop from site *i* to site *j* is given by[22]

$$P_{ij} = \omega_0 e^{(E_i - E_j)/2T}. \tag{2}$$

Here, ω_0 stands for the bare hopping frequency, T is the temperature, while E_i and E_j denote site energies.

The mobilities of electrons and holes usually differ by orders of magnitude in materials used for OLEDs. It is reasonable to treat one type of carrier as immobile (target), while the carrier of the other type is approaching. This approximation was adopted both by Gartstein *et al.* for the recombination in bulk and by Greenham and Bobbert for the two-dimensional (2D) treatment of heterojunction. In rare cases where the mobilities may be comparable, one can generalize the model by considering the relative motion of the electron and the hole. For the heterojunction problem, the relative motion that should be considered is that parallel to the heterojunction plane, because the energy barriers that electrons and holes experience at the heterojunction (LUMO energy difference for electrons and HOMO difference for holes) are usually quite different. Therefore, the motion perpendicular to the heterojunction is blocked for at least one type of carrier. In the present paper, we choose the hole as the immobile target, being stuck on its side of the heterojunction,[35] as shown in Fig. 1.

We assume that the electrons are homogeneously injected at the left-hand side of the box in Fig. 1(b).[36] They move under the influence of the externally applied homogeneous electric field and the electric field of holes in the device. Those electrons that do not recombine leave the box on its right-hand side. The hole is positioned at the central site of the grid, immediately after the heterojunction. At the sides of the box that are perpendicular to the heterojunction plane, we impose periodic boundary conditions. Thus, an electron pouring out through one side of the box pours in through the opposite side. Such conditions also imply periodicity of targets (holes), which form a square lattice in the heterojunction plane.[37] The size of the box in the direction parallel to the heterojunction determines the planar concentration of the holes at the heterojunction $p=1/(Na)^2$. We emphasize that we do not intend to dwell on all of the intricacies of a full device model, which would include discussing injection at the electrodes and the space charge effects in the bulk. Instead, we focus solely on the physics of the organic-organic interface.

There are two special sites in the grid shown in Fig. 1(b). One, denoted by *T* in material B right after the heterojunction, is occupied by the immobile hole. The other site, denoted by *P*, is the site in material A nearest to *T*. Electrons that arrive at the *T* or *P* site can form exciton or exciplex states, respectively (exci*T*on or exci*P*lex, hence the notation), and can recombine from that state.[38] The fraction of electrons that recombine defines the *recombination probability* P_{rec}. We calculate the total cross section σ_{tot} from $P_{rec} = \sigma_{tot} p$. The quantity $1-\sigma_{tot} p$ is the fraction of the electrons that exit the device without recombining. The ratio of the electrons that recombine in the exciton or the exciplex channel defines the respective partial cross sections: σ_T and σ_P ($\sigma_T + \sigma_P = \sigma_{tot}$). For small values of the recombination probability $P_{rec} \ll 1$, σ_{tot}, σ_T, and σ_P, thus defined, agree with the usual notion of a cross section. We extend this definition to larger values of the recombination probability $P_{rec} \sim 1$, where the magnitude of these cross sections is influenced by finite size effects. Notably, the value of the total cross section σ_{tot} cannot exceed $(Na)^2$. These "size effects" are physical; they represent the influence of other holes on the heterojunction, which compete for the same electron. So it is this extension of the cross section that is relevant at finite densities.

The calculation of the cross section by Gartstein *et al.* relied on the Monte Carlo method. An objective of the Monte Carlo approach is to extract a proper sample of trajectories of an electron injected into the system.[13] This approach is rather straightforward but may become computationally demanding.[16,39] An alternative approach is to consider an ensemble of electrons exploring *all* possible paths through the system. This second approach leads to a master equation, where all possible paths are simultaneously accounted for.[40]

Within the master equation approach, one solves for the probabilities n_i of an electron visiting site i. These probabilities, also termed "densities," determine the average hopping current J_{ij} from site i to site j through

$$J_{ij} = n_i P_{ij} - n_j P_{ji}. \tag{3}$$

The average currents J_{ij} flowing from some site i are related through the local continuity equation

$$\sum_j J_{ij} = 0. \tag{4}$$

This equation holds for every site where electrons come and leave exclusively through hopping. Exceptions occur at sites T and P, where we also allow for recombination. There, the recombination process contributes an additional term and the equations become

$$\sum_j J_{Tj} - n_T \gamma_T = 0, \tag{5}$$

$$\sum_j J_{Pj} - n_P \gamma_P = 0, \tag{6}$$

for the T and P sites, respectively. Here, γ_T and γ_P represent the decay rates (inverse of recombination lifetimes) of the exciton and exciplex states. It is generally considered that $\gamma_T \gg \gamma_P$, since the recombination of an exciplex involves the off-site hop of an electron. Once close to the hole, at the same or at the neighboring molecule, the probability for the electron to detach and leave is considered to be low, except at extremely high electric fields. Indeed, our calculations show that the total cross section σ_{tot} is independent of γ_T for a wide range of values. In the following calculations, we use $\gamma_T = 500\omega_0$, which forces rapid recombination once an electron reaches T site. Also, if not stated otherwise, we use $\gamma_T/\gamma_P = 2500$. As we will show later, our results manifest no qualitative change when γ_P is varied over several orders of magnitude.

Equations (4)–(6) and (3) form a set of $N^2 N_x$ linear equations for n_i's. In our calculations, this amounts to over 2×10^5 equations. Due to the short-range nature of the hopping process, these can be efficiently solved using modern sparse matrix techniques.[41–43]

The site energy E_i that enters Eq. (2) depends on the LUMO energy $E_{LUMO,i}$ of the molecule at site i as well as on the externally applied electric field F and the shift U_i in the carrier's energy due to other carriers in the system:

$$E_i = E_{LUMO,i} - q_e F x_i + U_i. \tag{7}$$

Here, q_e is the elementary charge and x_i is the coordinate of site i in the direction perpendicular to the heterojunction. Field F is assumed to be oriented in the opposite direction. The mean value of $E_{LUMO,i}$ in materials A and B are denoted as E^A_{LUMO} and E^B_{LUMO}, respectively. The difference

$$\Delta_0 = E^B_{LUMO} - E^A_{LUMO} \tag{8}$$

represents the energy barrier that electrons experience at the heterojunction. Apart from this jump at the heterojunction, LUMO energies are taken either as constant within a given material or experiencing some site-energy disorder,

$$E_{LUMO,i} = E_{LUMO} + \delta\epsilon_i. \tag{9}$$

We assume $\delta\epsilon_i$ to be a "dipolar" correlated disorder, as introduced by Parris and co-workers[22,23] and supported by mobility studies. The strength of disorder is denoted by $\Sigma_D = \langle (\delta\epsilon_i)^2 \rangle^{1/2}$. The spatial correlation of $\delta\epsilon_i$ is given[22] with $\langle (\delta\epsilon_i)(\delta\epsilon_j) \rangle \propto 1/r_{ij}$ for $r_{ij} \gg a$.

The main contribution to the energy shift U_i comes from the hole at site T, within the same box as the electron under consideration. At a distance r_{iT} far from the T site, $r_{iT} \gg a$; this contribution is just the Coulomb energy $U_i \approx -q_e^2/4\pi\varepsilon_0\varepsilon_r r_{iT}$. At shorter distances, the finite extension of molecular orbitals and the quantum effects influence U_i, which then loses the simple $1/r_{iT}$ dependence. In particular, at the T site, U_T is finite and is given by the exciton binding energy for a molecule of material B, $U_T = -E^T_{bind}$. Similarly, at the P site occupied by a molecule of material A, it is given by the exciplex binding energy[44] $U_P = -E^P_{bind}$. We encompass and simplify all of the cases by using

$$u(r) = -\frac{1}{4\pi\varepsilon_0\varepsilon_r} \frac{q_e^2}{\sqrt{r^2 + a^2}} \tag{10}$$

to describe the contribution to U_i of a single hole at distance r from the i site. This embodies the behavior at large distances and the regularization of the $1/r$ divergence close to the hole. This may seem to be a coarse simplification, but it turns out that there are a few properties of U_i at small distances that qualitatively matter, the most important being the difference of the binding energies of the exciton and exciplex, $u(a) - u(0) = E^T_{bind} - E^P_{bind}$. To incorporate the influence of other nearby holes at the heterojunction, Coulomb potentials of the holes in the surrounding eight boxes (see Fig. 1) are also added to U_i. Contributions from further holes are neglected and are approximately canceled by contributions of electrons in their respective boxes.

For the relative dielectric constant of the medium, we choose $\varepsilon_r = 3$, which is appropriate for materials used in OLEDs. If not stated otherwise, the grid used in the calculation contains 60^3 sites. The lattice constant of $a = 6$ Å is used, which is comparable to the size of organic molecules used in OLEDs. The thickness of $N_x a = 60a$ is of the order of those used in real devices. $N = 60$ corresponds to the surface density of holes $p = 7.716 \times 10^{-10}$ cm^{-2}. The effect of the hole density at the heterojunction on the recombination will be studied by varying N.

III. RESULTS

A. Space distribution of carriers and currents

The most direct way to perceive the qualitative features of our results is by visualizing the flow of the electrons for typical values of parameters. Figures 2–4 illustrate the flow for several typical cases. The flow lines are constructed as trajectories by treating the quantity J_{ij}/n_i as a local "fluid" velocity and by interpolating the flow between sites. Therefore, these lines do not represent the actual movement of the carriers, which is stochastic, but, rather, the average flow. In

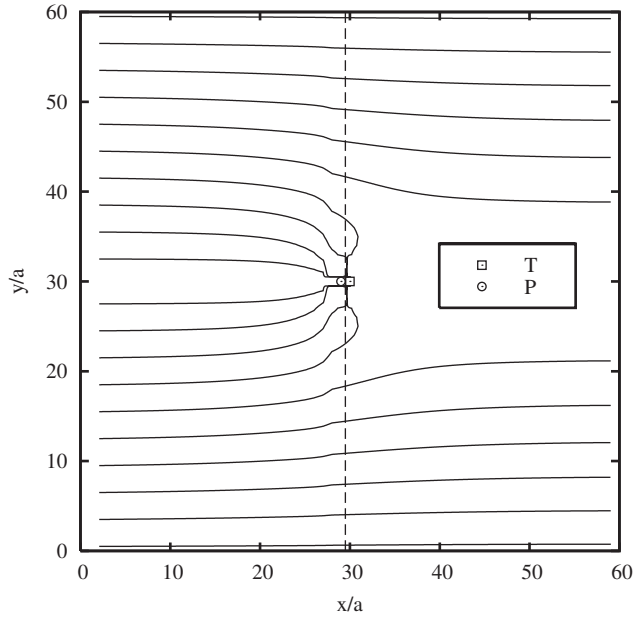

FIG. 2. Average flow of electrons for a low energy barrier (Δ_0 =0.04 eV). The T and P sites are marked by a square and circle, respectively. Flow lines are only lightly perturbed by the attraction originating from the hole, and by the heterojunction, except in proximity of the hole. The value for the recombination cross section is close to the one obtained in the bulk. The electric field of 0.4 MV/cm is directed along the x axis.

these figures, the recombination cross section can be roughly estimated from the fraction of the lines starting at the left-hand side and ending at either the T or the P site. Numerically, the cross section is calculated either from the difference of the inflow and outflow of electrons or directly from $n\gamma$ terms in Eqs. (5) and (6).

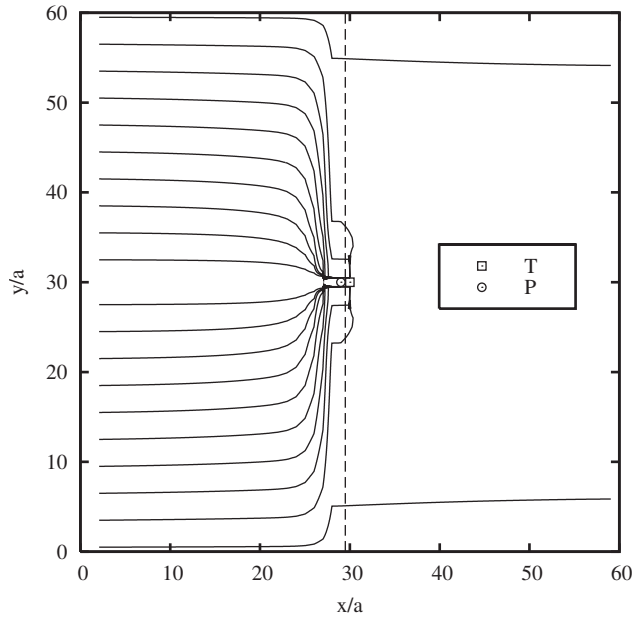

FIG. 3. Flow lines for a somewhat higher barrier of Δ_0 =0.20 eV. Virtually all flow lines end at site P. However, as in the case of weak barrier (Fig. 2), they only slightly deviate from straight lines until almost reaching the heterojunction. F =0.4 MV/cm.

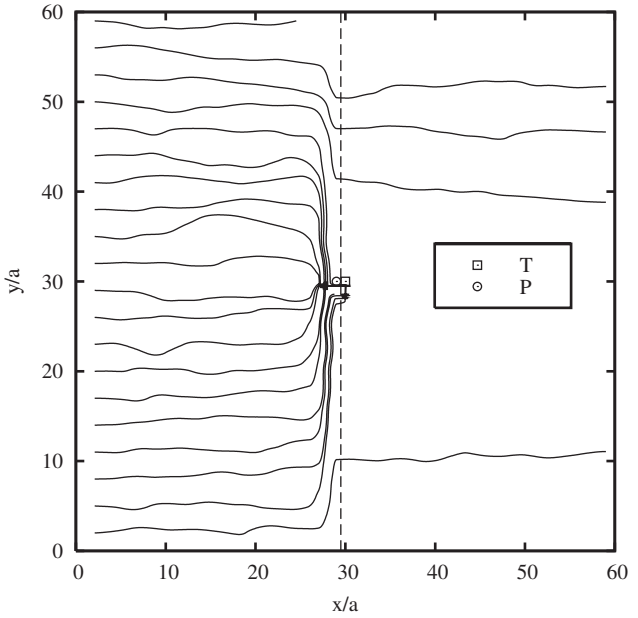

FIG. 4. Flow lines in an energetically disordered system (Σ_D =0.03 eV). The barrier is Δ_0=0.21 eV and the field is F =0.8 MV/cm. The general features of the flow are essentially the same as in the case without disorder (Fig. 3). Note that the (x,z) plane shown in the figure is not the plane of exact symmetry anymore, since disorder forces the flow out of and into the plane. For simplicity, the y component of the current has been neglected in preparing the 2D graphs shown here, resulting in an approximate illustration of the flow.

As can be seen in the figures, the flow before the heterojunction is almost unperturbed by the Coulomb field of the hole, except in proximity to the heterojunction. Deviation starts a few monolayers prior to the heterojunction, where a substantial fraction of the incoming current diverts "radially" toward the hole, affected by its electric field. The fraction of current that is radially diverted depends on the height of the energy barrier (cf. Figs. 2 and 3). In the case of a high barrier, most of the electrons finish recombining at either the P or T site. The flow of carriers in this case seems to justify the 2D approximation of Greenham and Bobbert. As the barrier is lowered, a substantial fraction of carriers crosses the heterojunction early enough to "leak out" from the device unrecombined. The height of the barrier that they cross is position dependent

$$\Delta(r) = \Delta_0 - q_e F a - [u(r) - u(\sqrt{r^2 + a^2})], \qquad (11)$$

with r denoting the distance from the center of the heterojunction plane in Fig. 1. The last term, representing the interaction of the electron and hole, is particularly significant for sites in the neighborhood of the P site. For intermediate to low values of Δ_0, this term opens a "gate" in the barrier in the vicinity of the P site. The gate represents the part of the heterojunction where no barrier exists for electrons, $\Delta(r) < 0$. Keeping in mind the physical meaning of $u(a)$ and $u(0)$, the requirement for opening of the gate may be expressed

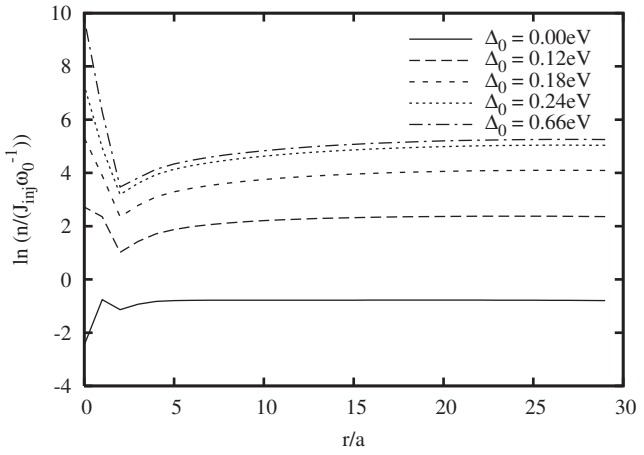

FIG. 5. Logarithm of electron density in the preheterojunction monolayer α, plotted as a function of the distance r from the P site. Graphs for various values of the energy barrier Δ_0 are normalized to the density J_{inj} of the current injected at the cathode. Except in proximity of the center (site P), the observed variation of $n(r)$ is small. In the proximity of site P, the density is lower than elsewhere for low barriers, and significantly bigger than elsewhere for very high barriers, reflecting the increasing stability of the exciplex state. $F=0.8$ MV/cm.

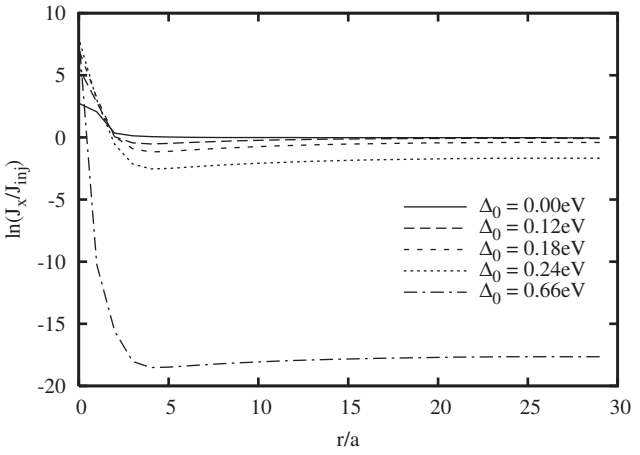

FIG. 6. Logarithm of the density of the current through the heterojunction as a function of the distance from the center. The contribution from the exciplex recombination is also included at $r=0$. As the barrier rises, the portion of current that flows from P to T increases, mostly in the form of an exciplex recombination. The field strength is $F=0.8$ MV/cm.

through exciton and exciplex binding energies, $\Delta_0 - q_e F a < \Delta_{0c}$, where

$$\Delta_{0c} \equiv E_{bind}^{T} - E_{bind}^{P}. \tag{12}$$

For the parametrization used in the simulation, Δ_{0c} corresponds to 0.23 eV. The existence of the gate essentially marks the instability of the exciplex toward the creation of the exciton. For larger values of $\Delta_0 - q_e F a$, the gate closes, leading to a stable exciplex state and raising the fraction of the recombination in the exciplex channel.

Unlike those before the heterojunction, the flow lines beyond the heterojunction remain unaltered by the barrier. Therefore, the electrons that cross the heterojunction at distances bigger than $\sqrt{\sigma_L/2\pi}$ are likely to escape recombination.[45] At those distances, the heterojunction current J_x consists mostly of electrons that leak out at the anode. This may be difficult to observe in Figs. 2 and 3 as the fraction of carriers that take those paths is small.

Figure 4 shows the flow in the presence of site-energy disorder. The flow lines are disturbed by disorder to some extent, but the picture remains qualitatively unaltered with respect to the one without disorder. The effects of disorder are addressed in more detail in later sections.

We focus first on the case without disorder. This case is illustrated in Figs. 5–7. The data refer to the preheterojunction monolayer α of Fig. 1(b). The density $n(r)$ and components of the current density are shown for several values of the energy barrier Δ_0, normalized to J_{inj}—the current density of electrons injected at the cathode. The variation of $n(r)$, as can be seen in Fig. 5, is small except in the proximity of the P site. The low variation of the density in the preheterojunction monolayer α coincides with a rather homogeneous "leak current" J_x through the heterojunction, as seen in Fig. 6. A small variation of the density also indicates that the radial current before the heterojunction consists mostly of the drift component.

These observations can be readily related through the continuity equation. Assuming homogeneous inflow J_{inj} to the heterojunction, homogeneous current J_x through the heterojunction, and radial symmetry in the heterojunction plane, the radial component $J_{rad}(r)$ of the current density must satisfy the continuity equation

$$\frac{d}{dr}[2\pi r a J_{rad}(r)] = 2\pi r (J_{inj} - J_x). \tag{13}$$

Upon integrating this equation from r to the distance r_c where J_{rad} vanishes, one obtains

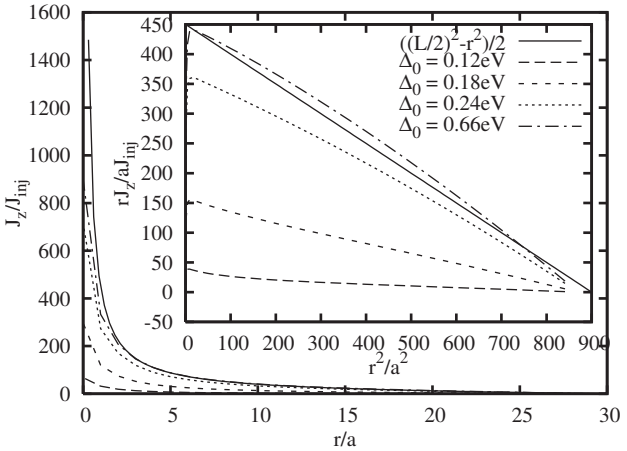

FIG. 7. Radial-current density in the preheterojunction plane α and the same current density multiplied by the distance from the center r, as a function of r^2 (inset). As explained in the text, the deviation from the $[(Na/2)^2 - r^2]/2$ line in the inset is due to the leak current through the barrier. The latter clearly decreases as the barrier is raised, and practically vanishes for barriers above 0.6 eV. The field strength is $F=0.8$ MV/cm.

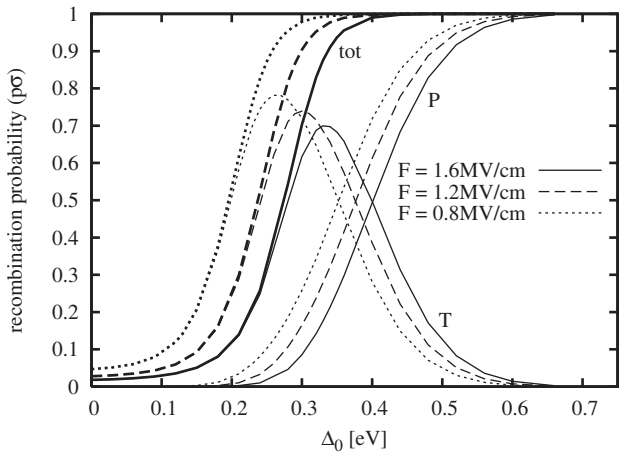

FIG. 8. Dependence of total and partial recombination probabilities $p\sigma$ on the bare energy barrier Δ_0 for three values of the applied electric field. Thick lines, labeled "tot," are used for the total recombination probability $p\sigma_{tot}$, while thinner lines, labeled "T" and "P," correspond to the partial recombination probabilities in the exciton and exciplex channels, $p\sigma_T$ and $p\sigma_P$. The recombination in the exciton channel exhibits a maximum at medium values of the barrier.

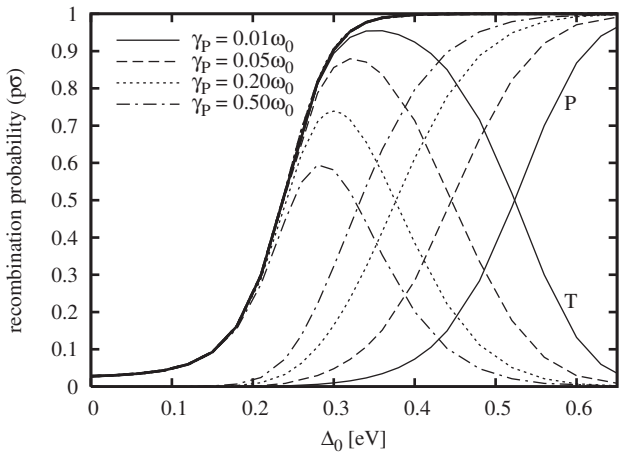

FIG. 9. Recombination probabilities $p\sigma_{tot}$, $p\sigma_T$, and $p\sigma_P$ versus the barrier height Δ_0 for several values of the exciplex decay rates γ_P. The total cross section does not vary with γ_P, but the maximum in the exciton cross section is stronger and wider for lower values of γ_P. The field strength is $F=1.2$ MV/cm.

$$\frac{rJ_{rad}(r)}{J_{inj}} = \frac{1}{2}\frac{J_{inj}-J_x}{J_{inj}}[r_c^2 - r^2]. \tag{14}$$

The distance r_c marks the midpoint between two holes, $r_c \sim Na/2$. Equation (14) implies that $rJ_{rad}(r)/J_{inj}$ is linear in r^2, with inclination that deviates from 1/2 as the magnitude of J_x increases. The relation fits our data rather well, as seen in Fig. 7. This is in spite of the violation of radial symmetry toward the edges of the rectangular box in Fig. 1.

B. Dependence of the cross section on the barrier height Δ_0

The height Δ_0 of the barrier at the heterojunction is directly related to the choice of materials used for the device. The device efficiency and the shape of emitted spectrum were found to depend on Δ_0.[46] This has been mainly ascribed to the interplay of excitons and exciplexes. This issue received very limited theoretical attention in models developed to simulate OLEDs. This was due to the difficulty of accounting for the strong correlation of electrons and holes at the heterojunction within the effective one-dimensional device models. The results of our simulations that address a wide range of Δ_0 are shown in Fig. 8. The figure shows the total and the partial cross sections for recombination in the exciton and exciplex channels as functions of the barrier height Δ_0 for three values of the applied electric field. The total cross section σ_{tot} starts, at low barriers, from a value close to σ_L. This limit will be discussed in more detail in Sec. III D. As Δ_0 increases, the total cross section σ_{tot} rapidly grows. We identify this growth as a rise of the recombination in the exciton channel, since $\sigma_{tot} \approx \sigma_T$ for small values of Δ_0. Dominance of the exciton channel is due to the instability of the exciplex state toward exciton formation when $\Delta(0)<0$. As Δ_0 is further increased, the exciplex stabilizes with $\Delta(0)>0$, and the recombination in the exciplex channel strongly takes over the one in the exciton channel. For large values of Δ_0, the total recombination cross section saturates at the value of $(Na)^2$, determined by target density p. At that point, all incoming carriers recombine. Experimentally, the crossover from exciton-dominated to exciplex-dominated recombination is not necessarily related to a strong change in shape of the spectrum of emitted light, since exciplexes generally poorly contribute to the light emission.[46,47] A strong impact of the crossover is expected, and observed, in the efficiency of an electroluminescent device. In fact, the whole dependence of σ_T on device parameters is expected to be directly reflected in efficiency. The appearance of a maximum in σ_T in Fig. 8 is a particularly important consequence of this crossover.[46] For applied electric fields around 1 MV/cm, the maxima in σ_T appear for Δ_0 in the range between 0.2 and 0.4 eV. At weaker fields, the optimal value of Δ_0 decreases and the maximal value of σ_T increases.

C. Effect of the exciplex decay rate γ_P

In Fig. 9, we compare the cross sections for different values of the exciplex decay rate γ_P. The dependence on the barrier height Δ_0 is shown for γ_P values ranging over 2 orders of magnitude. The shapes of the curves $\sigma_{tot}p$, $\sigma_T p$, and $\sigma_P p$ remain qualitatively the same throughout this range. Furthermore, the total cross section σ_{tot} is insensitive to changes in γ_P. This is to be expected; all electrons reaching the proximity of the hole recombine in one way or another, as the probability for escape is rather low. Hence, a change of γ_P only affects the ratio σ_T/σ_P. A weaker γ_P produces a stronger maximum in the exciton cross section σ_T, and the corresponding peak becomes much wider in Δ_0.

The observed behavior can be well described by a simple formula. We start from an assumption, suggested by the shape of flow lines in the system with a barrier, that the electrons recombining on the T site mostly arrive there through the P site. Thus, the probability n_P of the P site being occupied determines both the probability for decay in

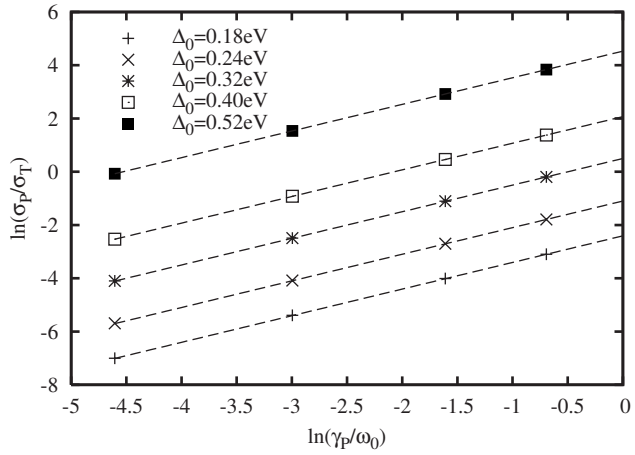

FIG. 10. Exciplex-to-exciton recombination ratio σ_P/σ_T as a function of exciplex decay rate γ_P (log-log plot). Dashed lines, which are the best fits to data, all have an inclination of 1. The offsets that these lines make on the vertical axis equal $\Delta/2T$ to within 10% deviation. The field strength is $F=1.2$ MV/cm.

the exciplex channel and the flow to the T site that results in the creation of an exciton. n_P cancels out when the ratio of two processes is considered, giving

$$\frac{\sigma_P}{\sigma_T} = \frac{\gamma_P}{\omega_0} \exp\left(\frac{\Delta(0)}{2T}\right). \tag{15}$$

This equation suggests that the ratio σ_P/σ_T is linear in γ_P. Numerical simulations confirm this in a wide range of Δ_0 and γ_P/ω_0 values, as shown in Fig. 10. Thus, the assumption is validated; a large majority of electrons that reach the hole use the P site to cross the heterojunction. In other words, the occurrence of the exciton state is strongly correlated with the assistance of one type of carrier to another in crossing the heterojunction.

D. Dependence of the cross section on the strength of the applied electric field

Of all the parameters, the field strength is the one most easily adjustable in reality, simply by varying the applied voltage. Thus, the cross section's field dependence can be thought of as a good indicator of the actual voltage characteristic of a device. Caution should be exercised, however, as the local field at a heterojunction need not scale linearly with the device voltage. Furthermore, we calculate the cross sections at a constant density of holes. In reality, this density changes with voltage, affected by the injection characteristics of the anode and the cathode. We shall not deal with such complications here, as they are out of the scope of the present paper.

By setting $\Delta_0=0$, we can simulate the recombination in the bulk, thereby essentially repeating the approach and recovering the results of the former Monte Carlo simulations[13] (Fig. 11). In particular, we reproduce the sublinear dependence of the cross section on inverse electric field. As discussed in Ref. 13, this deviation from the linear dependence found for σ_L is caused by the field-dependent mobility that

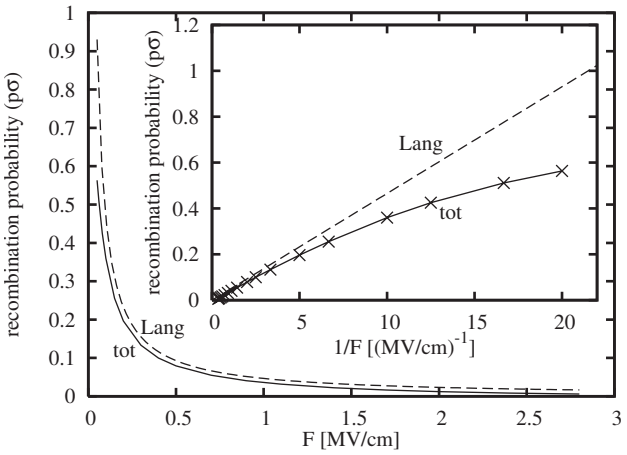

FIG. 11. Dependence of the recombination probability on the field strength for zero barrier ($\Delta_0=0$) and small p. The full line is $p\sigma_{tot}$ calculated from the model, and the dashed line is the Langevin recombination probability $p\sigma_L$. The inlet shows the dependence on the inverse field. We get the same sublinear behavior as found in Ref. 13, related to the choice of the hopping law in a discrete system.

follows from the hopping law appropriate for an organic molecular medium.

The situation changes when the heterojunction is present, as shown in Fig. 12. For low fields and high barriers, the recombination probability saturates at unity. At high fields, the effective barrier $\Delta_0 - q_e Fa$ is lowered, and the total cross section drops, thus approaching the behavior found in the bulk.

For high enough barriers ($\Delta_0 > \Delta_{0c}$), the dependence of the exciton cross section σ_T on electric field develops a maximum. On the low-field side of the maximum, the exciton cross section is dominated by the lowering of the effective barrier with rising electric field. This increases the recombination in the exciton channel at the expense of the recombination in the exciplex channel, as described by Eq.

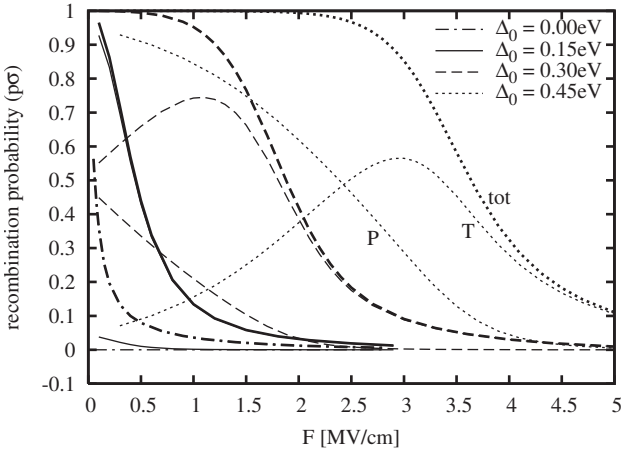

FIG. 12. Dependence of the recombination probability on field strength for several barrier heights. Symbols (see Fig. 8) are placed near the family of lines obtained for $\Delta_0=0.45$ eV. At barriers higher than 0.2 eV, the exciton cross section exhibits a maximum at nonzero field strengths.

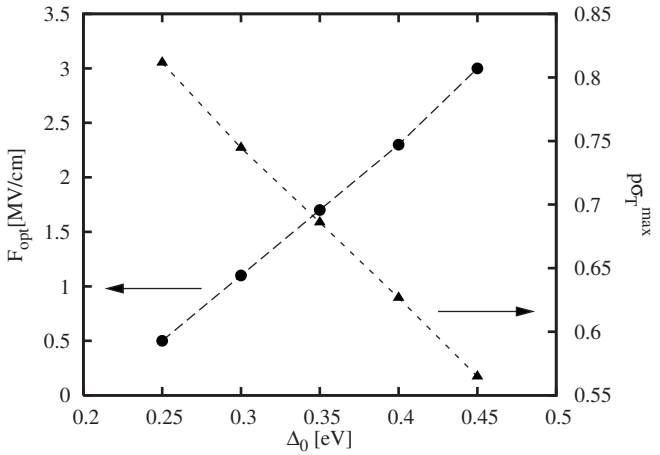

FIG. 13. Optimal field values F_{opt} (circles) at which the exciton cross section shows a maximal value (see Fig. 12), and the corresponding maxima of exciton recombination probabilities $p\sigma_T^{max}$ (triangles) for various barrier heights Δ_0. For barriers lower than 0.25 eV, the optimal field cannot be distinguished from zero. The grid size (inverse target density) is $60a \times 60a$.

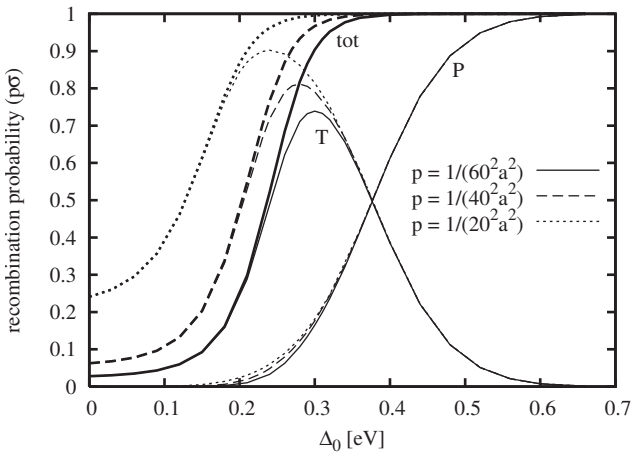

FIG. 14. Total and partial recombination probabilities for three values of the planar density of holes at the heterojunction, $p = 1/(Na)^2$. The strength of the applied electric field is $F = 1.2$ MV/cm.

(15). At high fields, the decrease of σ_T follows the fall of the total cross section. Figure 12 shows this maximum shifting to higher fields and decreasing in intensity as the barrier rises.

Figure 13 summarizes the behavior of the maximum as a function of the barrier. Both the maximal value of σ_T and the optimal electric field F_{opt} appear linear in Δ_0.

One may be inclined to compare the existence of the maxima in the exciton channel in Fig. 12 to the occurrence of maxima in experimental measurements of quantum efficiency versus bias voltage in multilayer OLEDs.[47–50] This comparison is complicated by the fact that, experimentally, voltage simultaneously affects the electric field and the density of carriers at the heterojunction. The latter is related to the properties of electrodes, which we presently do not consider. However, the dependence on the density of holes at the heterojunction is considered separately in the next section.

E. Effect of the surface density of targets

The density of the holes at the heterojunction can be affected by the strength of the applied electric field. The choice of materials used in OLED affects the injection characteristics of the electrodes, likewise shifting the balance of carriers at the heterojunction. In our simulation, the variation of the planar density p of holes at the heterojunction is accomplished by varying the size N of the box in the direction perpendicular to the applied electric field ($p = 1/(Na)^2$). Figure 14 shows the recombination probabilities as functions of Δ_0 for three values of p: $1/(20a)^2$, $1/(40a)^2$, and $1/(60a)^2$. For $a = 0.6$ nm, these densities are respectively 69.44×10^{-10}, 17.36×10^{-10}, and 7.716×10^{-10} cm^{-2}. The maximum in the exciton channel grows and shifts to lower barriers as the density of holes increases. Although it is expected for the recombination probability to increase as the concentration of holes rises, the observed gain appears minor: the maximal efficiency changes only by some 25% when the density of holes is altered by approximately 1 order of magnitude. Exactly the opposite behavior is found in Fig. 14 for the recombination probability in the $\Delta_0 \to 0$ limit, which scales linearly with the concentration of holes. The constant of proportionality is given by the "sub-Langevin" value of σ_{tot}, previously discussed in relation to Fig. 11. It may be reasoned that a rather weak dependence of the maximal value of the exciton cross section on the concentration of holes is a consequence of the sharp rise of total cross section with increasing barrier. Since the maximum of the recombination probability in the exciton channel always occurs in the regime in which the total probability for recombination is already close to unity, little room is left for an additional variation with the concentration of holes.

Another related feature, also visible in Fig. 14, is that the lines corresponding to the recombination probability in the exciplex channel show no variation with the concentration of holes. This follows from the fact that, for the examined range of concentrations p, the exciplex cross section also becomes noticeable only in the regime in which the total recombination probability saturates, $p\sigma_{tot} \sim 1$. In that regime, $p\sigma_P = p\sigma_{tot}/(1 - \sigma_T/\sigma_P) \approx 1/(1 - \sigma_T/\sigma_P)$. This is independent of the concentration p of holes, as can be seen from Eq. (15). The dependence of the recombination probability in the exciplex channel on the density of holes is expected to be more pronounced in the limit of a very low density of holes.

F. Influence of the disorder

We separately investigated two forms in which disorder can manifest: the site-energy disorder and the roughness of the heterojunction surface. The site-energy disorder is implemented through a spatially correlated random potential $\delta\epsilon_i$, calculated from randomly oriented dipoles, attached to molecular sites, as in Ref. 22. A rough heterojunction was implemented by randomly varying the x coordinate of the boundary between materials A and B by one or more molecular layers, thus creating "bumps" and "pits" on the heterojunction surface. For each type and strength of disorder, we

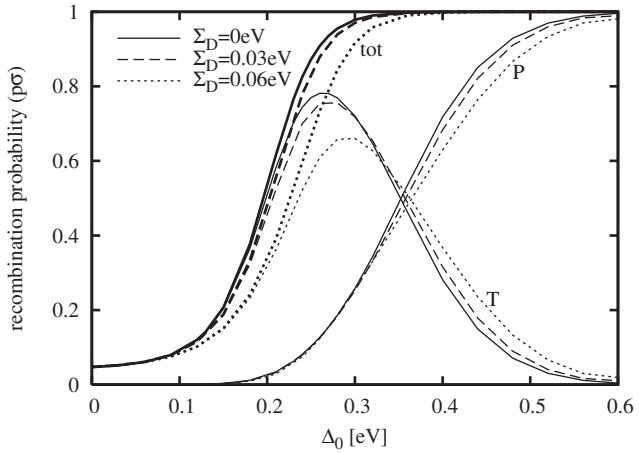

FIG. 15. Dependence of the recombination probabilities on barrier height in systems with a spatially correlated site-energy disorder for different disorder strengths Σ_D. A reduction in the total cross section as well as a reduction in the maxima in the exciton channel are noticeable. The field strength is $F=0.8$ MV/cm.

consider several realizations of the disordered system. Typically, six random configurations are used to produce average values and estimate scattering (not shown in the following figures). The scattering tends to be small for the total cross section, but quite pronounced for the partial cross sections. This is expected, since the choice between recombination in the exciton and exciplex channels is made once the electron arrives at the P site, and thus depends on the local value of the barrier. On the other hand, the total cross section $\sigma_T + \sigma_P$ is determined by the probability of the electron reaching the P site in the first place, and thus reflects the average barrier the electron experiences on its path along the heterojunction surface.

In Fig. 15, we present a comparison of the cross sections for site-energy disorders with an energy variance Σ_D of 0.03 and 0.06 eV, as well as for the ordered case. The introduction of dipolar site-energy disorder lowers the total cross section, stretching the curve to higher values of Δ_0. The maximum in the exciton channel is reduced in value and also shifted to higher barriers. The overall decrease in cross section is related to the reduced mobility in the preheterojunction plane caused by disorder. This implies a longer time for carriers to reach the target, consequently amplifying the probability to leak through the barrier.[15] The latter probability is further magnified by "cracks" in the energy barrier, statistically introduced by site-energy disorder,[32] where the barrier is lowered and hopping rates through the heterojunction wall are strongly increased.

In the case of structural disorder, the surface of the heterojunction contains bumps and pits. These can be viewed as another form of site-energy disorder on a two-dimensional surface, as the applied field creates an energy difference, $q_e F \delta x_i$, between monolayers. We assume that the hole has settled in one of the protruding bumps, which is energetically most favorable in the presence of an external electric field. An immediate consequence is the increased number of sites involved in the formation of an exciplex, as illustrated in Fig. 16.

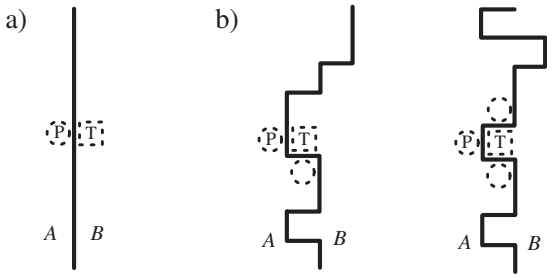

FIG. 16. Close-up view of the neighborhood of the target, perpendicular to the heterojunction. Squares and circles mark the sites where the exciton and exciplex recombination takes place, respectively. (a) Shows a smooth heterojunction surface, with only one exciplex recombination site present (notably, the P site). (b) Shows two out of many possible configurations for a rough, two-monolayer-wide, heterojunction surface, where more than one site is available for the exciplex formation and recombination.

In Fig. 17, we present the results for rough interfaces extending over one and two molecular layers. For one layer and for an applied field of 0.8 MV/cm, the variation of the term $q_e F x_i$ at the heterojunction is about 0.02 eV. For a rough heterojunction extending over two molecular layers, this variation doubles to 0.04 eV. These values are comparable to the site-energy disorder considered previously. Nevertheless, the reduction in the total cross section is substantially bigger for the rough heterojunction surface in Fig. 17 than for the corresponding site-energy disorder in Fig. 15. The partial cross section in the exciton channel is particularly reduced. We conclude that the roughness of the heterojunction surface has a much stronger impact on the formation of excitons and the electroluminescence than the site-energy disorder within the organic media does. This result is an

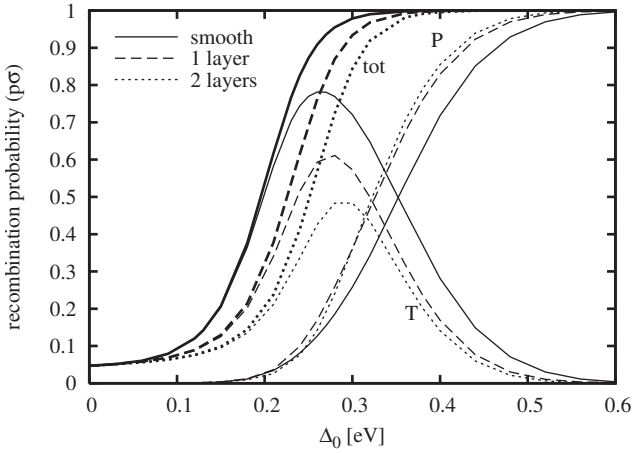

FIG. 17. Dependence of recombination probabilities on the energy barrier for structurally disordered (rough) heterojunctions. "Smooth" means a smooth heterojunction surface, while "1 layer" and "2 layer" stand for a rough, bumpy surface, with bumps extending to one or two monolayers. The total cross section is reduced more than for comparable values of site-energy disorder (see Fig. 15). The rough surface also allows for more sites to be involved in the formation of exciplexes, leading to higher cross sections in the exciplex channel and significantly reduced cross section for excitons. The field strength is $F=0.8$ MV/cm.

example of how the details of molecular arrangement at the heterojunction may affect the spectra in OLEDs. Another such example is the effect of stacking disorder at the heterojunction on excitons, recently investigated in some polymeric bilayers.[28,29,51]

IV. CONCLUSIONS

We have performed three-dimensional simulations of recombination at the heterojunction under the applied field, recreating conditions found in OLED devices. As the energy barrier at the heterojunction rises, the motion of the electrons and holes across the heterojunction surface becomes increasingly important. The crossing of the heterojunction by one carrier type is then dominated by sites where the carriers of opposite sign can assist. This amplifies the probability of recombination, first in the exciton and then, as the barrier further rises, in the exciplex channel. We found a simple relation between the cross sections in the exciplex and exciton channels, which applies for a wide range of device parameters. It portrays well the maxima we found for the recombination in the exciton channel, regarded either as a function of barrier height or applied electric field. Since excitons usually have a larger light yield, such maxima represent OLEDs with optimal efficiency. We have also investigated the influence of the site-energy disorder and the roughness of the organic-organic interface. We found that roughness has a much stronger impact than site-energy disorder, especially on the relative probability for the creation of excitons or exciplexes.

This paper presents numerical simulations concentrating on the heterojunction problem. The next step is to incorporate our findings into a full model for a multilayer device in which the injection, the transport of both types of carriers, the space charge effects, and the recombination in the bulk appear on equal footing with the heterojunction physics.

Greenham and Bobbert already discussed one important consequence of different modelings of the heterojunction, namely, the overcharging of the heterojunction, by comparing the outputs of two numerical models for a simple bilayer device.[15] Further corrections to the device model, proposed in this paper, relate to the renormalization of the recombination cross section and the renormalization of barriers in the exciton and exciplex channels. The inclusion of these is expected to further enhance the modeling of multilayer devices, which has, nonetheless, been fairly successful in reproducing many experimental features in OLEDs.[52–56] In view of the present paper, the success of prior models partly stems from the fact that the current-voltage characteristic in multilayers with a blocking heterojunction depends dominantly on the injection at electrodes.[57] Second, the simulations have been compared against experiments mostly for devices for which the energy barrier (either for the electrons or for the holes) is rather low.[52–55,57] Even so, the comparisons showed a necessity for a significant barrier renormalization. This was especially apparent in the simulations of the charging transients, since the transients directly reveal the charge accumulation at the heterojunction.[54] The need for the barrier renormalization was less evident in the simulations of the steady state, where its absence was roughly compensated by the large underestimate of the cross section. This compensation worked rather well for devices with high recombination efficiency. At the same time, the spurious accumulation of both types of carriers, confined to the heterojunction region, did not influence the electric field distribution elsewhere in the device.[57,58] Meanwhile, the exciplex recombination due to accumulated charges could not manifest, as it was *ad hoc* turned off in the models.

The proper renormalization of the recombination cross section and the proper calculation of the barrier height relevant for exciplex and exciton creation eliminate these problems, thus creating the opportunity for modeling devices with high heterojunction barriers. However, the efficient device models should not rely on three-dimensional simulations.[59] Instead, good approximate formulas accounting for the effects found in our three-dimensional simulation should be developed and used in an effective one-dimensional device model. This work is in progress.

ACKNOWLEDGMENTS

Useful discussions with D. Berner, M. Castellani, and H. Houili are gratefully acknowledged. The work presented in this paper is supported by the Croatian Ministry of Science, Education and Sports, under Grant No. 035-0352826-2847.

*ijuric@ifs.hr
†edo@ifs.hr

[1] C. W. Tang and S. A. VanSlyke, Appl. Phys. Lett. **51**, 913 (1987).
[2] H. Bässler, Phys. Status Solidi B **175**, 15 (1993).
[3] L. B. Schein, D. Glatz, and J. C. Scott, Phys. Rev. Lett. **65**, 472 (1990).
[4] L. B. Schein, Philos. Mag. B **65**, 795 (1992).
[5] D. H. Dunlap and V. M. Kenkre, Chem. Phys. **178**, 67 (1993).
[6] L. Zuppiroli, M. N. Bussac, S. Paschen, O. Chauvet, and L. Forro, Phys. Rev. B **50**, 5196 (1994).
[7] Yu. N. Gartstein and E. M. Conwell, Chem. Phys. Lett. **217**, 41 (1994).
[8] M. N. Bussac, D. Michoud, E. Tutiš, and L. Zuppiroli, Proc. SPIE **3476**, 156 (1998).
[9] E. A. Silinsh, in *Electrical and Related Properties of Organic Solids*, edited by R. W. Munn, A. Miniewicz, and B. Kuchta (Springer, New York, 1997), pp. 133–156.
[10] S. Forrest, Nature (London) **428**, 911 (2004).
[11] P. Langevin, Ann. Chim. Phys. **28**, 287 (1903); **28**, 433 (1903).
[12] J. C. Scott, P. J. Brock, J. R. Salem, S. Ramos, G. G. Malliaras, S. A. Carter, and L. Bozano, Synth. Met. **111-112**, 289 (2000).
[13] Y. N. Gartstein, E. M. Conwell, and M. J. Rice, Chem. Phys. Lett. **249**, 451 (1996).

[14] Coulomb interaction among the carriers, if taken at mean field level, does not essentially modify this picture.
[15] N. C. Greenham and P. A. Bobbert, Phys. Rev. B **68**, 245301 (2003).
[16] Z. G. Yu, D. L. Smith, A. Saxena, R. L. Martin, and A. R. Bishop, Phys. Rev. B **63**, 085202 (2001).
[17] R. W. Munn, A. Miniewicz, and B. Kuchta, *Electrical and Related Properties of Organic Solids* (Springer, New York, 1997) provides a valuable collection of relevant reviews.
[18] B. Ries and H. Bässler, Phys. Rev. B **35**, 2295 (1987).
[19] P. M. Borsenberger, L. T. Pautmeier, and H. Bässler, Phys. Rev. B **46**, 12145 (1992).
[20] P. E. Parris, V. M. Kenkre, and D. H. Dunlap, Phys. Rev. Lett. **87**, 126601 (2001).
[21] Yu. N. Gartstein and E. M. Conwell, Chem. Phys. Lett. **245**, 351 (1995).
[22] D. H. Dunlap, P. E. Parris, and V. M. Kenkre, Phys. Rev. Lett. **77**, 542 (1996).
[23] S. V. Novikov, D. H. Dunlap, V. M. Kenkre, P. E. Parris, and A. V. Vannikov, Phys. Rev. Lett. **81**, 4472 (1998).
[24] I. I. Fishchuk, D. Hertel, H. Bässler, and A. K. Kadashchuk, Phys. Rev. B **65**, 125201 (2002).
[25] L. Pautmeier, R. Richert, and H. Bässler, Philos. Mag. B **63**, 587 (1991).
[26] M. N. Bussac, J. D. Picon, and L. Zuppiroli, Europhys. Lett. **66**, 392 (2004).
[27] C. Madigan and V. Bulović, Phys. Rev. Lett. **97**, 216402 (2006).
[28] P. Sreearunothai, A. C. Morteani, I. Avilov, J. Cornil, D. Beljonne, R. H. Friend, R. T. Phillips, C. Silva, and L. M. Herz, Phys. Rev. Lett. **96**, 117403 (2006).
[29] J. G. S. Ramon and E. R. Bittner, J. Chem. Phys. **126**, 181101 (2007).
[30] H. Houili, E. Tutiš, I. Batistić, and L. Zuppiroli, J. Appl. Phys. **100**, 033702 (2006).
[31] H. Houili, E. Tutiš, and L. Zuppiroli, Synth. Met. **156**, 1256 (2006).
[32] E. Tutiš, I. Batistić, and D. Berner, Phys. Rev. B **70**, 161202(R) (2004).
[33] E. Tutiš and I. Batistić, Fiz. A **14**, 167 (2005).
[34] In the Miller-Abrahams model, the hopping probability P_{ij} equals $\omega_0 e^{-(E_i-E_j)/T}$ when $E_i<E_j$, and ω_0 when $E_i>E_j$.
[35] If at least one type of carriers is not blocked at the heterojunction, the barrier would be effectively nonexistent, the case not of interest in this paper.
[36] This is a fairly safe assumption for contacts with good injection characteristics, although the injection can be rather inhomogeneous in real devices, as pointed out in Refs. 32 and 60. In the latter case, the equivalent assumption is that inhomogeneities at the anode and at the cathode are not correlated, and may be separately averaged over.
[37] Of course, in reality, the holes at the heterojunction do not form a regular lattice. Our aim here is to account for their finite density at the heterojunction. The external electric field pushes the holes toward the heterojunction, while the Coulomb repulsion between them tends to keep them apart.
[38] We neglect the possibility of tunneling recombination from farther sites, corresponding to a weakly bound *electroplex* (Ref. 61) state. Distinction between an exciplex and a strongly bound electroplex is moot, both in their theoretical description (Refs. 62 and 63) and in their luminescence spectra (Ref. 63). Thus, the exciplex state that we refer to in this paper can be considered to encompass both, with binding energy E_{bind}^{P} including both the electrostatic interaction and the quantum correlations.
[39] For problems where probabilities for certain processes are very low, one has to generate many or extremely long trajectories in order to obtain proper statistics within the Monte Carlo approach. This is especially true for the heterojunction problem with high barriers. However, high barriers present no particular problem within the master equation approach.
[40] The master equation turns advantageous for an ensemble of single electrons. However, considering more than one electron moving through the system simultaneously turns difficult within the master equation approach. Physically, this type of calculation is required when Coulomb interaction among the same type of carriers is sizable, usually for carrier densities well above those found in OLEDs. The multiparticle Monte Carlo method that we have developed previously (Ref. 30) becomes preferable in that case.
[41] O. Schenk and K. Gärtner, Future Generation Comp. Syst. **20**, 475 (2004).
[42] O. Schenk and K. Gärtner, Electron. Trans. Numer. Anal. **23**, 158 (2006).
[43] G. Karypis and V. Kumar, SIAM J. Sci. Comput. (USA) **20**, 359 (1998).
[44] We do not make a distinction between triplet and singlet excited states with regards to their energy, leaving possible effects of spin on the transport through the heterojunction for further studies.
[45] The analytical solution of the flow for vanishing barrier $\Delta_0 \to 0$ and constant mobility shows that the separatrise between flow lines that end at site T and those that leave the device passes the heterojunction plane at distance $\sqrt{\sigma_L/2\pi}$ from the target site.
[46] M. Castellani and D. Berner, J. Appl. Phys. **102**, 024509 (2007).
[47] C. Giebeler, H. Antoniadis, D. D. C. Bradley, and Y. Shirota, J. Appl. Phys. **85**, 608 (1999).
[48] K. Itano, H. Ogawa, and Y. Shirota, Appl. Phys. Lett. **72**, 636 (1998).
[49] M. Cocchi, D. Virgili, G. Giro, V. Fattori, P. D. Marco, J. Kalinowski, and Y. Shirota, Appl. Phys. Lett. **80**, 2401 (2002).
[50] G. He, O. Schneider, D. Qin, X. Zhou, M. Pfeiffer, and K. Leo, J. Appl. Phys. **95**, 5773 (2004).
[51] The mechanism proposed in Refs. 28 and 29 for the observed blueshift involves excitons probing the charge distribution of neutral molecules in different materials, as well as a frequency-dependent transfer of excitations between two materials. At the phenomenological level, this can be partially modeled within our framework, but lies beyond the scope of the present paper.
[52] J. Staudigel, M. Stössel, F. Steuber, and J. Simmerer, J. Appl. Phys. **86**, 3895 (1999).
[53] E. Tutiš, M. N. Bussac, B. Masenelli, M. Carrard, and L. Zuppiroli, J. Appl. Phys. **89**, 430 (2001).
[54] B. Ruhstaller, S. A. Carter, S. Barth, H. Riel, W. Riess, and J. C. Scott, J. Appl. Phys. **89**, 4575 (2001).
[55] A. B. Walker, A. Kambili, and S. J. Martin, J. Phys.: Condens. Matter **14**, 9825 (2002).
[56] H. Houili, E. Tutiš, H. Lütjens, M. N. Bussac, and L. Zuppiroli, Comput. Phys. Commun. **156**, 108 (2003).
[57] E. Tutiš, D. Berner, and L. Zuppiroli, J. Appl. Phys. **93**, 4594 (2003).
[58] S. J. Martin, G. L. B. Verschoor, M. A. Webster, and A. B.

Walker, Org. Electron. **3**, 129 (2002).
[59] A multiparticle Monte Carlo approach that has been recently developed, in principle, could serve for the purpose of three-dimensional device modeling (Ref. 30). Although very helpful in the investigation of some focused issues, this tool is impractical for routine device simulations, and rather demanding in computer resources.
[60] E. Tutiš, D. Berner, and L. Zuppiroli, Proc. SPIE **5465**, 330 (2004).
[61] T. Granlund, L. A. A. Pettersson, M. R. Anderson, and O. Inganäs, J. Appl. Phys. **81**, 8097 (1997).
[62] M. Cocchi, D. Virgili, C. Sabatini, and J. Kalinowski, Chem. Phys. Lett. **421**, 351 (2006).
[63] S. Yang, X. Zhang, Y. Hou, Z. Deng, and X. Xu, J. Appl. Phys. **101**, 096101 (2007).